ChemPubSoc Europe

DOI: 10.1002/chem.201501614

CHEMISTRY A European Journal Communication

Metal–Organic Frameworks

Redox-Active Metal–Organic Frameworks: Highly Stable Charge-Separated States through Strut/Guest-to-Strut Electron Transfer

Nivedita Sikdar,[a] Kolleboyina Jayaramulu,[a] Venkayala Kiran,[b] K. Venkata Rao,[c] Srinivasan Sampath,[b] Subi J. George,*[c] and Tapas Kumar Maji*[a, c]

Abstract: Molecular organization of donor and acceptor chromophores in self-assembled materials is of paramount interest in the field of photovoltaics or mimicry of natural light-harvesting systems. With this in mind, a redox-active porous interpenetrated metal–organic framework (MOF), $\{[Cd(bpdc)(bpNDI)]\cdot 4.5\,H_2O\cdot DMF\}_n$ (**1**) has been constructed from a mixed chromophoric system. The μ-oxo-bridged secondary building unit, $\{Cd_2(\mu\text{-}OCO)_2\}$, guides the parallel alignment of bpNDI (*N,N*′-di(4-pyridyl)-1,4,5,8-naphthalenediimide) acceptor linkers, which are tethered with bpdc ($bpdcH_2 = 4,4'$-biphenyldicarboxylic acid) linkers of another entangled net in the framework, resulting in photochromic behaviour through inter-net electron transfer. Encapsulation of electron-donating aromatic molecules in the electron-deficient channels of **1** leads to a perfect donor–acceptor co-facial organization, resulting in long-lived charge-separated states of bpNDI. Furthermore, **1** and guest encapsulated species are characterised through electrochemical studies for understanding of their redox properties.

The spatial organization of organic chromophores in self-assembled scaffolds is important for understanding and controlling the processes in artificial light-harvesting systems and in various optoelectronic devices.[1] However, the development of such supramolecular organizations that can harvest visible light and guide excitation energy or electron transfer in a controlled manner impose a real challenge. Recently, the perception of photofunctional metal–organic frameworks (MOFs) with chromophoric linkers as an organised matrix of light harvesters has moved to the fore.[2] The concept of crystal engineering and reticular chemistry based on predesigned organic linkers and secondary building units (SBU) allows the desired spatial organization of organic chromophores in MOFs and, hence, the intermolecular distances and angles between the organic linkers can be controlled.[3] MOFs have already drawn substantial attention for their potential applications in several fields, such as gas storage, separation, catalysis and drug delivery, based on their permanent porosity.[4] However, the well-defined nanopores provide additional design potential for incorporating chromophoric guest molecules to modulate the photophysical processes.[5] This design has been extensively used for light harvesting in MOFs with tuneable luminescent properties.[2a,e,5c] On the other hand, redox-active multichromophoric frameworks that exhibit electron transfer between the linkers or with guest molecules have been underexplored. Such a design would give extended donor–acceptor arrays with specific organization, which would exhibit interesting charge-transport or ferroelectric properties or may act as shape-selective sensors.[6] Although co-facial donor–acceptor assemblies, which often lead to partial charge-transfer complexes, are well studied, achieving complete electron transfer requires better control of the spatial organization of the molecular components.[1c] In this respect, we envisaged that mixed chromophoric MOFs can be useful for grafting suitable donors (D) and acceptors (A) with long range order. Entanglement of frameworks would be one of the strategies for achieving close contacts of D and A chromophoric linkers to realise photoinduced charge or electron transfer.

For this purpose, we have turned our attention to the aromatic redox-active naphthalenediimides (NDIs). NDIs are planar, chemically robust and easily reducible molecules that have been utilised as efficient electron-accepting chromophores (n-type) in different applications, such as in photosynthesis, solar energy conversion, electrochromic devices, molecular electronics, and as photochromic materials.[7] We have chosen a pyridine-substituted NDI derivative, that is, bpNDI (*N,N*′-di(4-pyridyl)-1,4,5,8-naphthalenediimide) as the pillar[8] and $bpdcH_2$ (4,4′-biphenyldicarboxylic acid) as the linker for the construction of a novel redox-active framework $\{[Cd(bpdc)(bpNDI)]\cdot 4.5\,H_2O\cdot DMF\}_n$ (**1**), which is a twofold interpenetrated 3D multichromophoric porous framework. In this communication, we show that this framework exhibits unique photochromic behaviour resulting from the long-lived charge-separated chromophores, as a result of inter-net strut-to-strut electron transfer (Scheme 1). Furthermore, encapsulation of

[a] *N. Sikdar, Dr. K. Jayaramulu, Prof. T. K. Maji*
Chemistry and Physics of Materials Unit
Jawaharlal Nehru Centre for Advanced Scientific Research
Bangalore-560064 (India)
E-mail: tmaji@jncasr.ac.in

[b] *Dr. V. Kiran, Prof. S. Sampath*
Department of Inorganic and Physical Chemistry
Indian Institute of Science (IISc), Bangalore-560012 (India)

[c] *Dr. K. V. Rao, Prof. S. J. George, Prof. T. K. Maji*
New Chemistry Unit
Jawaharlal Nehru Centre for Advanced Scientific Research
Bangalore-560064 (India)
E-mail: george@jncasr.ac.in

Supporting information for this article is available on the WWW under http://dx.doi.org/10.1002/chem.201501614.

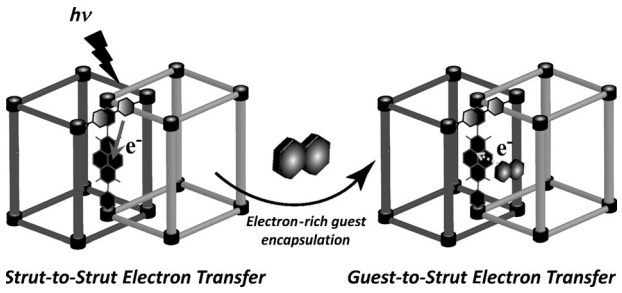

Scheme 1. Schematic diagram of the ground-state strut-to-strut/guest-to-strut electron transfer in multichromophoric redox-active interpenetrated 3D framework, **1**.

electron-rich guest molecules [for example, 1,5-/2,6-dinaphthol (1,5/2,6-DAN) and 4,*N*,*N*-trimethylaniline (DMPT)] into the electron-deficient channels of this framework leads to very stable charge-separated states in the ground state. Although, NDI and dinaphthols are a well-known charge-transfer pair,[7f,g] this is the first report of the incorporation of them into a MOF that results in the formation of a highly stable bpNDI radical anion by complete electron transfer.

The compound **1** was synthesised by using solvothermal conditions and single-crystal X-ray diffraction analysis suggests that **1** crystallises in the monoclinic $P2_1/n$ space group. The Cd^{II} metal centre is heptacoordinated and two such metal centres form a $\{Cd_2(\mu_2\text{-}OCO)_2\}_n$ SBU and these SBUs are connected by bpdc linkers to form an extended 2D rhombic network along the $(10\bar{1})$ plane (Figure 1a). This 2D layer is further bipillared by bpNDI linkers to form a (2,8)-c connected 3D framework

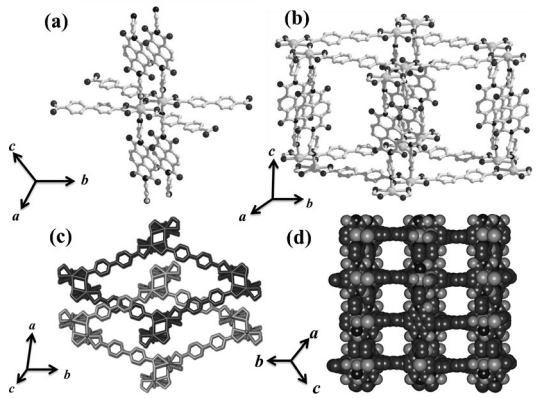

Figure 1. Crystal structure of **1**: a) coordination environment of Cd^{II} with $\{Cd_2(\mu_2\text{-}OCO)_2\}_n$ SBU; b) 3D bipillared-layer framework; c) twofold interpenetration along crystallographic *c*-axis; d) pore view along crystallographic $[10\bar{1}]$ direction.

structure (Figure 1b). It is worth mentioning that the μ_2-oxo bridged dinuclear SBU ensures the two bpNDI units stack in a face-to-face fashion (cg···cg distance $\approx$3.844 Å), resulting in a bipillared layer framework. The NDI cores of the pillar bpNDI linkers maintain the perfect parallel arrangement with respect to each other (the dihedral angle between the NDI cores is 0°). However, the pyridine ring of bpNDI is not in the same plane as the NDI core and the corresponding tilting angle between them is 58.32°. Moreover, the presence of long linkers results in a large void space in the 3D net and, hence, induces twofold interpenetration in the framework (Figure 1c). Upon interpenetration, the framework shows a 1D rectangular channel with dimensions of 6.4×7.1 Å^2 along the $[10\bar{1}]$ direction (Figure 1d); the channel is filled with guest water and DMF molecules.

Thermogravimetric analysis (TGA) showed that the guest molecules are removed in a stepwise manner (in the temperature range 55–240 °C, Figure S1 in the Supporting Information) and the desolvated state of **1** (**1**′) remains stable up to 345 °C. The powder X-ray diffraction (PXRD) pattern of **1**′ (Figure 2a) shows no distinct change compared with that of **1**, suggesting a robust nature of the framework. As seen from the single-crys-

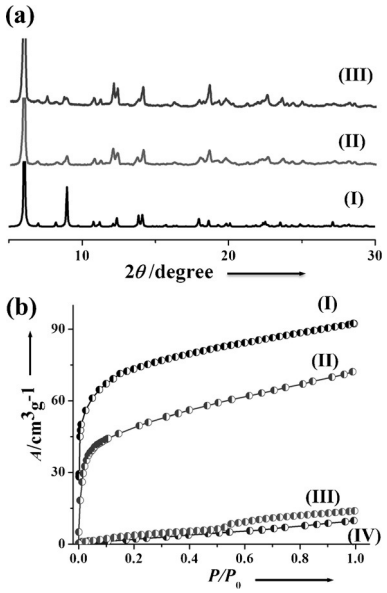

Figure 2. a) PXRD patterns of **1** in different states: (I) simulated, (II) as-synthesised **1**, (III) desolvated **1** (**1**′); b) CO_2 adsorption isotherms at 195 K: (I) **1**′, (II) **1@DMPT**, (III) **1@1,5-DAN** and (IV) **1@2,6-DAN**.

tal structure, **1** contains a high amount of void space, but it does not show any N_2 uptake at 77 K (Figure S2 in the Supporting Information). This might be due to the low thermal energy of the adsorbate relative to the high diffusion barrier as the framework contains a 1D channel structure.[9] However, CO_2 adsorption measurements at 195 K showed a typical type I profile (Figure 2b and Figure S2), unveiling the microporous nature of the framework. The saturated CO_2 uptake is 92 $cm^3 g^{-1}$ (18 wt%, 3.2 CO_2 molecules per formula unit), which corresponds to a Langmuir surface area of 286 $m^2 g^{-1}$. **1**′ is also able to capture CO_2 at 298 K at a relatively high value of 34 $cm^3 g^{-1}$ (6.8 wt%, 1.1 CO_2 per formula unit; Figure S2). The uptake of CO_2 in **1**′ can be accounted for by the quadrupolar nature of the CO_2 molecules (quadrupole moment of CO_2: 4.3×10^{26} esu^{-1} cm^{-2}), which interact with the pendent carbonyl oxygen atoms of the bpNDI pillars that are aligned along the pore surface.

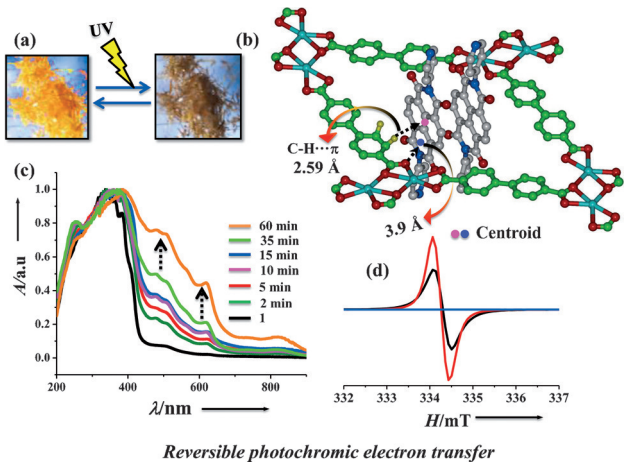

Figure 3. Reversible photoinduced strut-to-strut electron transfer: a) photographs of **1** before and after UV radiation (365 nm); b) possible supramolecular interactions between two different struts realised by interpenetration (cyan = Cd^{II}, red = oxygen, green = C atoms of bpdc, grey = C atoms of bpNDI, blue = N and yellow = hydrogen); c) UV/Vis time-dependent absorbance spectra on UV irradiation; d) EPR spectra of **1** (blue = **1** without irradiation, black = 3 min of irradiation, red = 7 min of irradiation).

The compound **1** shows broad absorption in the range of 200–400 nm, characteristic of typical π–π* and n–π* transitions. The presence of a very weak band in the visible region (400–600 nm) corresponds to π-stacked bpNDI chromophores, as is evident in the crystal structure as well. The origin of this band is further confirmed by the solution-state self-assembly studies of bpNDI chromophores in DMF/water solvent mixtures. A higher percentage of water induced aggregation of these chromophores, which resulted in similar features in absorption bands (Figure S3 in the Supporting Information). We further studied the photophysical responses of this framework upon exposure to UV-light irradiation, where two chromophores of different electronic nature are parts of the integrated framework. Interestingly, shinning UV light (365 nm) for as little as 20–30 s on crystals of **1** resulted in an immediate drastic colour change (Figure 3a and Figure S4 in the Supporting Information) from golden yellow to dark brown, while the crystal structure remained intact as supported by the PXRD pattern (Figure S5 in the Supporting Information). The colour of these crystals was reverted to yellow by keeping them in air for 7 to 8 h (Figure S6 in the Supporting Information). The UV/Vis spectra of irradiated crystals of **1** showed the appearance of new bands with maxima at 478, 617, 737 and 821 nm, the intensity of which increases on longer exposure to UV light (Figure 3c). The possible origin of these peaks is the formation of radical anions of the bpNDI linker molecules (see below). The formation of the radical anion is further confirmed by the chemical reduction of the bpNDI linker with *tert*-butylammonium fluoride and by comparing the corresponding UV/Vis spectra (Figure S7 in the Supporting Information).[10a] Appearance of a strong EPR signal with a *g* value of 2.001 for the irradiated crystals of **1** corroborates the formation of radical anions of bpNDI, where the radical is on the carbon atom (Figure 3d).[7e] On the other hand, free bpNDI ligands also showed similar photochromic behaviour (radical anion formation) upon UV irradiation owing to the intramolecular photoinduced electron transfer (PET) from the pyridine nitrogen to the NDI aromatic core (Figure S8 in the Supporting Information).[7e] The PET mechanism operating in the free bpNDI linkers is supported by the fact that the diprotonated $bpNDIH_2^{2+}$ showed no colour change upon irradiation. We envisage a similar diprotonated coordination environment for the bpNDI linker in framework **1** after binding with Cd^{II} and, hence, it is clear that the PET mechanism in the framework is quite different from that in the free linker molecule. Hence, we believe that the PET mechanism operating in the framework should be an intermolecular phenomenon, possibly between different strut molecules. Thus, control experiments were performed to understand the possible origins of the PET pathways. Interestingly, a 1:1 mixture of biphenyldicarboxylate ($bpdcNa_2$) with $bpNDIH_2^{2+}$ showed similar photochromic behaviour upon UV irradiation (Figures S9 and S10 in the Supporting Information). These linkers mimic the coordination environment of the framework and the formation of the radical ion was again confirmed by UV/Vis spectroscopy and EPR measurements (Figures S11 and S12 in the Supporting Information). It is important to note that UV irradiation of the $bpNDIH_2^{2+}$ and $bpdcH_2$ (1:1) mixture did not show any photochromic behaviour. These results clearly indicate that the photochromic behaviour in such systems is indeed due to an inter-strut photoinduced electron-transfer process and in the present case it is from the bpdc to the bpNDI acceptor linkers. This is only possible because of the perfect orientation of the struts in the framework, credited to the $\{Cd_2(\mu_2\text{-}OCO)_2\}_n$ SBU and the framework interpenetration, which causes close contacts of the struts (Figure 3b and Figure S13 in the Supporting Information). The donor component in this PET process can be either the carboxylate oxygen of the bpdc or the bpdc chromophoric linker itself, which are located at distances of 3.9 and 2.59 Å, respectively, from the electron-deficient bpNDI linker (Figure 3b).[10b] Although similar photochromic behaviour in NDI-based MOFs has been ascribed to a so called "π–π* electron transfer",[8d,e] we show here that the reduction of bpNDI acceptors to radical anions would indeed require a PET mechanism wherein the presence of an electron-donor group/molecule is mandatory.

Host–guest chemistry in luminescent porous MOFs is of great interest as various bimolecular photophysical properties, such as exciplex emission, charge-transfer or energy-transfer processes, can be modulated in a unique manner in the constrained spaces available inside the frameworks.[2,5] We further envisaged guest-induced modulation of the charge-transfer properties of this MOF with electron-deficient channels. Three different electron-rich guest molecules, that is, 4,*N*,*N*-trimethylaniline (DMPT) and 1,5-/2,6-dinaphthol (1,5-/2,6-DAN), were encapsulated successfully into **1**′ (**1@DMPT**, **1@1,5-DAN** and **1@2,6-DAN**) and striking colour changes were immediately observed, from golden yellow to dark brown, green and dark green, respectively, suggesting ground-state interactions between the host and guest chromophores (Figure 4a). The guest loading was confirmed through ^1H NMR (Figures S14–S16 in the Supporting Information), TGA (Figure S1), PXRD (Fig-

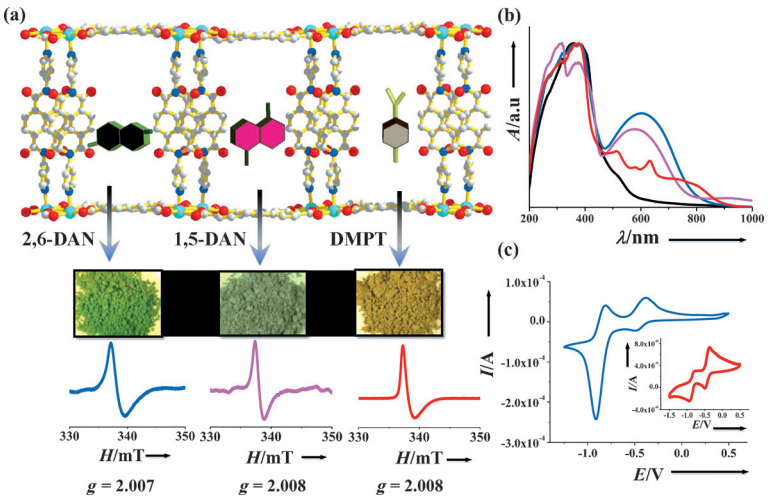

Figure 4. a) Encapsulation of electron-rich aromatic guest molecules (1,5-/2,6-DAN and DMPT) in **1**′ with corresponding colour change and EPR spectra (cyan = Cd^{II}, red = oxygen, grey = C atoms, blue = N); b) UV/Vis spectra of **1** and guest-encapsulated compounds (black = **1**, blue = **1@2,6-DAN**, purple = **1@1,5-DAN**, red = **1@DMPT** (100%)); c) cyclic voltammogram of **1@2,6-DAN** (inset: **1**) in 0.1 M TBAP in acetonitrile at a scan rate of 50 mV s^{-1}.

ure S17 in the Supporting Information) and elemental analyses. ^{1}H NMR spectra of the composites were recorded on digestion with DCl in [D_6]DMSO and confirmed that the percentages of guest loading per formula unit are 100, 90, 98% for **1@DMPT**, **1@1,5-DAN** and **1@2,6-DAN**, respectively. Changes in powder diffraction patterns of **1** on encapsulation also reiterate the successful loading of guest molecules. Furthermore, CO_2 adsorption isotherms (Figure 2b) for guest encapsulated composites **1@2,6-DAN** and **1@1,5-DAN** were measured at 195 K. As expected, both of the guest-loaded frameworks do not show any uptake of CO_2 up to 1 atm, unequivocally proving that 2,6/1,5-DAN occupy the regular channel of **1**. However, **1@DMPT** exhibits a type I profile with total CO_2 uptake of 72 $cm^3 g^{-1}$ (2.49 CO_2 molecules per formula unit), which is smaller than that of framework **1**′. It is probable that as DMPT is smaller in size than 2,6/1,5-DAN, there is sufficient void space for further CO_2 inclusion. The dark colours of the three composites are indicative of ground-state charge-transfer interactions and this is distinctly reflected in the appearance of broad bands in entire visible region of the UV/Vis spectra (Figure 4b). Specifically for **1@DMPT**, the bands are well resolved and the newly appeared bands at 513, 630, 728 and 792 nm can be attributed to the radical anion of bpNDI, suggesting a guest-to-host electron-transfer process. Furthermore, EPR measurements were carried out and strong EPR signals were obtained for each case, clearly confirming the fact of guest-to-host electron transfer (Figure 4a). Hence, it can be stated that the occlusion of suitable guest molecules in the functionalised channels gives rise to an extended co-facial arrangement between the guests and the pillars of the host, hence reflecting the importance of confinement effects in porous frameworks. It is worth mentioning that even after three to four months, the colour of the guest-encapsulated compounds do not change and the EPR signals remain the same, suggesting long-lived charge-separated states of bpNDI and guest molecules.

As the bpNDI linker is redox-active, electrochemical studies of frameworks **1** and **1@2,6-DAN** were performed to test their chemical change after guest inclusion on electrodes passing electrical energy.[7a,11] The cyclic voltammogram of pristine bpNDI exhibits two sets of fully reversible redox peaks that correspond to $[bpNDI]^{0/\bullet-}$ at $E_{1/2} = -0.52$ V and $[bpNDI]^{\bullet-/2-}$ at $E_{1/2} = -0.94$ V (Figure S18 in the Supporting Information). The redox peaks obtained in the case of pure bpNDI are retained even after formation of the MOF ($[bpNDI]^{0/\bullet-}$ at $E_{1/2} = -0.49$ V and $[bpNDI]^{\bullet-/2-}$ at $E_{1/2} = -0.94$ V), confirming that **1** is a redox-active porous framework (Table S4 in the Supporting Information and Figure 4c, inset). However, the feature is quasi-reversible in nature, unlike that of pristine bpNDI;[11] this might be due to the integrated bpNDI, electronic environment of which is not same as that of the free ligand. On the other hand, drastic changes in the voltammogram of guest-encapsulated **1@2,6-DAN** were observed compared with pristine bpNDI and **1** (Figure 4c). The very small current density of peak I ($[bpNDI]^{0/\bullet-}$ at $E_{1/2} = -0.49$ V) compared to peak II ($[bpNDI]^{\bullet-/2-}$ at $E_{1/2} = -0.91$ V) suggests that bpNDI is in a mono radical anion state formed by electron transfer from 2,6-DAN. The small current density of peak I suggests that minute amounts of bpNDIs are present in the system, but are not involved in the electron-transfer process. These results further suggest the role of the included guest (2,6-DAN) in the electron-transfer process in guest-loaded framework. The high peak current for peak II can be attributed to the combination of both electrochemical reduction and chemically generated mono anion radicals ($[bpNDI]^{0/\bullet-}$ and unreduced bpNDI linker. In the next step, the potential scan is inverted and the presence of two anodic peaks corresponds to the oxidation of $bpNDI^{2-}$ to $bpNDI^{\bullet-}$ followed by further oxidation of $bpNDI^{\bullet-}$ to bpNDI.

In conclusion, we have reported the synthesis and characterisation of a multichromophoric 3D interpenetrated redox-active porous framework with unique photoinduced inter-net strut-to-strut electron-transfer characteristics. Furthermore, electron-deficient and dynamic-coordination spaces enabled facile encapsulation of different electron-rich aromatic molecules, which results in strut-to-strut long-lived charge-separated states in the ground state. The unique ability of such multichromophoric system to encapsulate various guest molecules with an electron-transfer response holds great promise for designing novel functional redox-active materials. Therefore, such host materials can alter their physical and chemical properties in the presence of guest molecules in their cavities, thereby,

giving room for finding new phenomena with potential applications in sensing, charge-transport and photocatalysis.

Experimental Section

Synthesis of compound 1

A mixture containing $Cd(NO_3)_2 \cdot 4H_2O$ (0.1 mmol, 0.030 g), bpdc (0.1 mmol, 0.012 g) and bpNDI (0.05 mmol,0.021 g) was suspended in DMF (10 mL) in a 30 mL glass vial and heated at 80 °C for 3 days. The light-yellow needle-shaped crystals of **1** were collected after washing with DMF several times. Yield: 88%. Elemental analysis calcd (%) for $C_{82}O_{27}Cd_2H_{72}N_{10}$: C 53.59, H 3.81, N 7.62; found: C 53.53, H 3.76, N 7.60; FTIR (4000–400 cm^{-1}): 3358 (w), 3066 (w), 2925 (w), 1715 (s), 1675 (s), 1602 (w), 1577 (s), 1507 (w), 1395 (s), 1339 cm^{-1} (s).

Preparation of 1@2,6-DAN, 1@1,5-DAN and 1@DMPT

An activated sample of **1** (i.e.,**1**′, approximately 140 mg, 0.16 mmol) was stirred with a methanolic solution (8 mL) of 2,6-dinaphthol (2,6-DAN; 0.32 mmol for 98% inclusion), 1,5-dinaphthol (1,5-DAN, 0.32 mmol for 90% inclusion) or 4,*N*,*N*-trimethylaniline (DMPT) (0.32 mmol for 100% inclusion) for 3 days for encapsulation into the channels of **1**′. The resulting different guest-encapsulated compounds were collected, washed with MeOH 3 or 4 times to remove the 2,6-DAN, 1,5-DAN or DMPT molecules adsorbed on the surface of **1**′, then dried in open atmosphere and used for several experiments. The guest-encapsulated compounds were characterised by TGA (Figure S1), PXRD (Figure S17), NMR spectroscopy (Figures S14–S16) and elemental analyses, all of which suggest that 0.9, 0.98 and 1 molecule of 1,5-DAN, 2,6-DAN and DMPT, respectively, were encapsulated per formula unit of **1**′. The lower concentration of DMPT leads to 0.5 molecule encapsulation in **1**′.

1@DMPT: Elemental analysis calcd (%) for [$C_{38}O_8CdH_{20}N_4$, 1 DMPT, 2 H_2O]: C 64.84, H 3.97, N 7.76; found: C 64.82, H 4.89, N 7.70; FTIR (4000–400 cm^{-1}): 3387 (w), 3065 (w), 2899 (w), 1715 (s), 1671 (s), 1604 (w), 1576 (s), 1418 (w), 1395 (s), 1340 cm^{-1} (s).

1@1,5-DAN: Elemental analysis calcd (%) for [$C_{38}O_8CdH_{20}N_4$, 0.9 1,5-DAN, 1.5 H_2O]: C 64.25, H 3.14, N 6.14; found: C 64.21, H 3.10, N 7.81; FTIR (4000–400 cm^{-1}): 3408 (w), 3058 (w), 2823 (w), 1714 (s), 1672 (s), 1609 (w), 1579 (s), 1507 (s), 1487 (s), 1345 cm^{-1} (s).

1@2,6-DAN: Elemental analysis calcd (%) for [$C_{38}O_8CdH_{20}N_4$, 0.98 2,6-DAN]: C 64.31, H 3.64, N 6.14; found: C 64.30, H 3.62, N 6.10; FTIR (4000–400 cm^{-1}): 3401 (w), 3062 (w), 2918 (w), 1715 (s), 1680 (s), 1606 (w), 1573 (s), 1501 (w), 1390(s), 1329 cm^{-1} (s).

Physical measurements

Elemental analysis was carried out using a Thermo Fischer Flash 2000 Elemental Analyzer. IR spectra were recorded on a PerkinElmer UTAR with a Frontier IR system. Thermogravimetric analysis (TGA) was carried out on a Mettler Toledo TGA850 under a nitrogen atmosphere (flow rate = 50 mL min^{-1}) in the temperature range 30–700 °C (heating rate 3 °C min^{-1}). Powder XRD patterns of the compounds were recorded by using $Cu_{K\alpha}$ radiation (Bruker D8 Discover; 40 kV, 30 mA). Electronic absorption spectra were recorded on a PerkinElmer Lambda 900 UV-Vis-NIR Spectrometer and emission spectra were recorded on a PerkinElmer Ls 55 Luminescence Spectrometer. NMR spectra were obtained with a Bruker AVANCE 400 (400 MHz) Fourier transform NMR spectrometer with chemical shifts reported in parts per million (ppm). For EPR spectra measurements, a Bruker EMX spectrometer was used in the X-band operating at 9.43 GHz.

Electrochemical studies

All the electrochemical measurements were carried out using a CHI 660A electrochemical analyzer (CH instruments, USA). Electrochemical measurements were carried out with a conventional three-electrode system, wherein the compound-coated glassy carbon electrode acts as a working electrode and a large Pt foil and an Ag wire act as auxiliary and reference electrodes, respectively. A known amount (7 mg) of bpNDI/**1**/**1@2,6-DAN** was dispersed in 1 mL of ethanol and 20 μL of Nafion solution for 30 min. A 20 μL aliquot of the above dispersion was drop-cast onto the precleaned glassy carbon electrode and dried under ambient conditions for fabrication of the working electrode. Electrochemical measurements were performed in distilled acetonitrile under deaerated conditions. 0.1 M TBAP ($[(nBu)_4N]PF_6$) acted as the supporting electrolyte.

Acknowledgements

We thank Prof. S. V. Bhat, Bhagyashree K.S. and Lora Rita Goveas, Indian Institute of Science, Bangalore-560012 (India) for EPR measurements. N.S. acknowledges the Council of Scientific and Industrial Research (CSIR) and JNCASR for financial support. T.K.M. acknowledges CSIR, Govt. of India for funding.

Keywords: electron transfer · host–guest systems · metal–organic frameworks · photochromism · redox-active systems

[1] a) N. Kishi, M. Akita, M. Yoshizawa, *Angew. Chem. Int. Ed.* **2014**, *53*, 3604 – 3607; *Angew. Chem.* **2014**, *126*, 3678 – 3681; b) A. P. H. J. Schenning, E. W. Meijer, *Chem. Commun.* **2005**, 3245 – 3258; c) M. Kumar, K. V. Rao, S. J. George, *Phys. Chem. Chem. Phys.* **2014**, *16*, 1300 – 1313.

[2] a) M. V. Suresh, S. J. George, T. K. Maji, *Adv. Funct. Mater.* **2013**, *23*, 5585 – 5590; b) R. Haldar, K. V. Rao, S. J. George, T. K. Maji, *Chem. Eur. J.* **2012**, *18*, 5848 – 5852; c) C. Y. Lee, O. K. Farha, B. J. Hong, A. A. Sarjeant, S. T. Nguyen, J. T. Hupp, *J. Am. Chem. Soc.* **2011**, *133*, 15858 – 15861; d) T. Zhang, W. Lin, *Chem. Soc. Rev.* **2014**, *43*, 5982 – 5993; e) K. V. Rao, K. K. R. Datta, M. Eswaramoorthy, S. J. George, *Chem. Eur. J.* **2012**, *18*, 2184 – 2194; f) K. V. Rao, A. Jain, S. J. George, *J. Mater. Chem. C* **2014**, *2*, 3055 – 3064; g) Y. Cui, Y. Yue, G. Qian, B. Chen, *Chem. Rev.* **2012**, *112*, 1126 – 1162; h) C. Y. Sun, X. L. Wang, X. Zhang, C. Qin, P. Li, Z. M. Su, D. X. Zhu, G. G. Shan, K. Z. Shao, H. Wu, J. Li, *Nat. Commun.* **2013**, *4*, 2717 – 2725.

[3] a) M. Li, D. Li, M. O'Keeffe, O. M. Yaghi, *Chem. Rev.* **2014**, *114*, 1343 – 1370; b) T. Enoki, W. Lin, *Chem. Soc. Rev.* **2014**, *43*, 5982 – 5993.

[4] a) J. R. Li, J. Sculley, H. C. Zhou, *Chem. Rev.* **2012**, *112*, 869 – 932; b) L. E. Kreno, K. Leong, O. K. Farha, M. Allendorf, R. P. V. Duyne, J. T. Hupp, *Chem. Rev.* **2012**, *112*, 1105 – 1125; c) J. Shi, Y. Jiang, X. Wang, H. Wu, D. Yang, F. Pan, Y. Suad, Z. Jiang, *Chem. Soc. Rev.* **2014**, *43*, 5192 – 5210; d) M. Yoon, R. Srirambalaji, K. Kim, *Chem. Rev.* **2012**, *112*, 1196 – 1231; e) M. D. Allendorf, C. A. Bauer, R. K. Bhakta, R. J. T. Houk, *Chem. Soc. Rev.* **2009**, *38*, 1330 – 1352; f) S. Roy, A. Chakraborty, T. K. Maji, *Coord. Chem. Rev.* **2014**, *273*, 139 – 164; g) R. Haldar, S. K. Reddy, V. M. Suresh, S. Mohapatra, S. Balasubramanian, T. K. Maji, *Chem. Eur. J.* **2014**, *20*, 4347 – 4356; h) A. Hazra, S. Bonakala, S. K. Reddy, S. Balasubramanian, T. K. Maji, *Inorg. Chem.* **2013**, *52*, 11385 – 11397; i) R. Haldar, N. Sikdar, T. K. Maji, *Mater. Today* **2015**, *18*, 97 – 116; j) J. C. Tan, A. K. Cheetham, *Chem. Soc. Rev.* **2011**, *40*, 1059 – 1080; k) J. M. Taylor, R. Vaidhyanathan, S. S. Iremonger, G. K. H. Shimizu, *J. Am. Chem. Soc.* **2012**, *134*, 14338 – 14340.

[5] a) N. Yanai, K. Kitayama, Y. Hijikata, H. Sato, R. Matsuda, Y. Kubota, M. Takata, M. Mizuno, T. Uemura, S. Kitagawa, *Nat. Mater.* **2011**, *10*, 787 – 793; b) D. Tanaka, S. Horike, M. Ohba, M. Hasegawa, Y. Ozawac, K. Toriumi, S. Kitagawa, *Chem. Commun.* **2007**, 3142 – 3144; c) R. Haldar, R. Mat-

suda, S. Kitagawa, S. J. George, T. K. Maji, *Angew. Chem. Int. Ed.* **2014**, *53*, 11772 – 11777; *Angew. Chem.* **2014**, *126*, 11966 – 11971; d) H. Sato, R. Matsuda, K. Sugimoto, M. Takata, S. Kitagawa, *Nat. Mater.* **2010**, *9*, 661 – 666.

[6] a) T. Enoki, A. Miyazaki, *Chem. Rev.* **2004**, *104*, 5449 – 5478; b) Q. Ye, Y. Song, G. Wang, K. Chen, D. Fu, P. W. H. Chan, J. Zhu, S. D. Huang, R. Xiong, *J. Am. Chem. Soc.* **2006**, *128*, 6554 – 6555.

[7] a) G. Andric, J. F. Boas, A. M. Bond, G. D. Fallon, K. P. Ghiggino, C. F. Hogan, J. A. Hutchison, M. A. P. Lee, S. J. Langford, J. R. Pilbrow, G. J. Troup, C. P. Woodward, *Aust. J. Chem.* **2004**, *57*, 1011 – 1019; b) Z. Song, H. Zhan, Y. Zhou, *Angew. Chem. Int. Ed.* **2010**, *49*, 8444 – 8448; *Angew. Chem.* **2010**, *122*, 8622 – 8626; c) C. R. Wade, M. Li, M. Dincă, *Angew. Chem. Int. Ed.* **2013**, *52*, 13377 – 13381; *Angew. Chem.* **2013**, *125*, 13619 – 13623; d) Y. Wu, M. Frasconi, D. M. Gardner, P. R. McGonigal, S. T. Schneebeli, M. R. Wasielewski, J. F. Stoddart, *Angew. Chem. Int. Ed.* **2014**, *53*, 12860 – 12864; *Angew. Chem.* **2014**, *126*, 13074 – 13078; e) Y. Matsunaga, K. Goto, K. Kubono, K. Sako, T. Shinmyozu, *Chem. Eur. J.* **2014**, *20*, 7309 – 7316; f) T. Takada, Y. Otsuka, M. Nakamura, K. Yamana, *RSC Adv.* **2014**, *4*, 59440 – 59443; g) A. Das, M. R. Molla, B. Maity, D. Koley, S. Ghosh, *Chem. Eur. J.* **2012**, *18*, 9849 – 9859.

[8] a) Y. Takashima, V. M. Martínez, S. Furukawa, M. Kondo, S. Shimomura, H. Uehara, M. Nakahama, K. Sugimoto, S. Kitagawa, *Nat. Commun.* **2011**, *2*, 168 – 174; b) B. Q. Ma, K. L. Mulfort, J. T. Hupp, *Inorg. Chem.* **2005**, *44*, 4912 – 4914; c) V. M. Martínez-Martínez, S. Furukawa, Y. Takashima, I. L. Arbeloa, S. Kitagawa, *J. Phys. Chem. C* **2012**, *116*, 26084 – 26090; d) L. Han, L. Qin, L. Xu, Y. Zhou, J. Sunb, X. Zou, *Chem. Commun.* **2013**, *49*, 406 – 408; e) A. Mallick, B. Garai, M. Addicoat, P. S. Petkov, T. Heine, R. Banerjee, *Chem. Sci.* **2015**, *6*, 1420 – 1425; f) Y. Takashima, S. Furukawa, S. Kitagawa, *CrystEngComm* **2011**, *13*, 3360 – 3363.

[9] N. Sikdar, A. Hazra, T. K. Maji, *Inorg. Chem.* **2014**, *53*, 5993 – 6002.

[10] a) S. Guha, S. Saha, *J. Am. Chem. Soc.* **2010**, *132*, 17674 – 17677; b) Y. Zeng, Z. Fu, H. Chen, C. Liu, S. Liaoa, J. Dai, *Chem. Commun.* **2012**, *48*, 8114 – 8116.

[11] a) P. M. Usov, C. Fabian, D. M. D'Alessandro, *Chem. Commun.* **2012**, *48*, 3945 – 3947; b) C. F. Leong, B. Chan, T. B. Faust, P. Turner, D. M. D'Alessandro, *Inorg. Chem.* **2013**, *52*, 14246 – 14252.

Received: April 25, 2015
Published online on July 16, 2015